# Achieving Robustness to Aleatoric Uncertainty with Heteroscedastic Bayesian Optimisation

**Ryan-Rhys Griffiths**
Department of Physics
University of Cambridge
Cambridge, UK
rrg27@cam.ac.uk

**Miguel Garcia-Ortegon**
Department of Mathematics
University of Cambridge
Cambridge, UK
mg770@cam.ac.uk

**Alexander A. Aldrick**
Department of Physics
University of Cambridge
Cambridge, UK
av495@cam.ac.uk

**Alpha A. Lee**
Department of Physics
University of Cambridge
Cambridge, UK
aal44@cam.ac.uk

## Abstract

Bayesian optimisation is an important decision-making tool for high-stakes applications in drug discovery and materials design. An oft-overlooked modelling consideration however is the representation of input-dependent or heteroscedastic aleatoric uncertainty. The cost of misrepresenting this uncertainty as being homoscedastic could be high in drug discovery applications where neglecting heteroscedasticity in high throughput virtual screening could lead to a failed drug discovery program. In this paper, we propose a heteroscedastic Bayesian optimisation scheme which both represents and penalises aleatoric noise in the suggestions. Our scheme features a heteroscedastic Gaussian Process (GP) as the surrogate model in conjunction with two acquisition heuristics. First, we extend the augmented expected improvement (AEI) heuristic to the heteroscedastic setting and second, we introduce a new acquisition function, aleatoric-penalised expected improvement (ANPEI) based on a simple scalarisation of the performance and noise objective. Both methods penalise aleatoric noise in the suggestions and yield improved performance relative to a naive implementation of homoscedastic Bayesian optimisation on toy problems as well as a real-world optimisation problem.

## 1 Introduction

Bayesian optimisation is already being utilised to make decisions in high-stakes applications such as drug discovery [1, 2, 3, 4, 5], materials discovery [6, 7, 8], robotics [9], sensor placement [10] and tissue engineering [11]. In these problems heteroscedastic or input-dependent noise is rarely accounted for and the assumption of homoscedastic noise is often inappropriate. As a case study, heteroscedastic noise is the rule rather than the exception in the majority of scientific datasets. This is the case, not only in experimental datasets, but also in datasets where properties are predicted computationally. We illustrate this for molecular hydration free energies in Figure 1 using the dataset of [12] where there is a distribution of noise values and in general the noise function might be expected to grow in proportion to chemical complexity [13]. The consequences of neglecting heteroscedastic noise are illustrated using a second example in Figure 2. The homoscedastic model will underestimate noise in certain regions which could induce a Bayesian optimisation scheme to suggest values possessing large aleatoric noise. In an application such as high-throughput virtual

33rd Conference on Neural Information Processing Systems (NeurIPS 2019), Vancouver, Canada.

screening the cost of misrepresenting the noise during the screening process could amount to a year wasted in the physical synthesis of a drug [14].

In this paper we present a heteroscedastic Bayesian optimisation scheme capable of both representing and minimising aleatoric noise in the suggestions. Our contributions are:

1. The introduction of a novel combination of surrogate model and acquisition function designed to minimise heteroscedastic aleatoric uncertainty
2. A demonstration of our scheme's ability to outperform naive schemes based on homoscedastic Bayesian optimisation on toy problems in addition to a real-world optimisation problem
3. The provision of an open-source implementation of the model

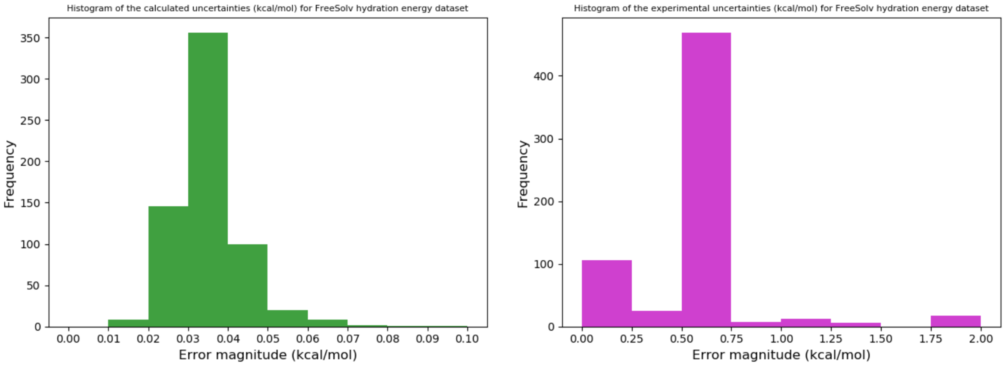

(a) Histogram of calculated uncertainties (b) Histogram of experimental uncertainties

Figure 1: Fig. (a) shows the frequency histogram of the calculated uncertainties against the error magnitude (kcal/mol) for the FreeSolv hydration energy dataset ([12]). Fig. (b) shows a similar plot for the experimental uncertainties.

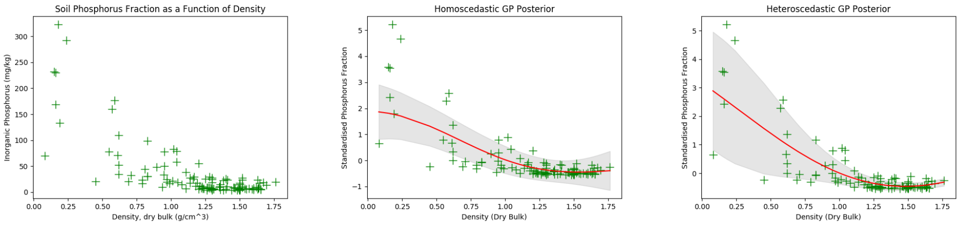

(a) Dataset (b) Homoscedastic GP Fit (c) Heteroscedastic GP Fit

Figure 2: Comparison of Homoscedastic and Heteroscedastic GP Fits to the Soil Phosphorus Fraction Dataset.

## 2 Related Work

The most similar work to our own is that of [15] where experiments are reported on a heteroscedastic Branin-Hoo function using the variational heteroscedastic GP approach of [16] although to the best of our knowledge this work does not consider sequential evaluations. [17] Introduce a modification to EI, expected risk improvement, that is applied to problems in robotics where robustness to aleatoric noise is desirable. [18, 19, 20] implement heteroscedastic Bayesian optimisation but don't introduce an acquisition function that penalises aleatoric uncertainty. [21, 22] consider the related problem of safe Bayesian optimisation through implementing constraints in parameter space. In this instance the goal of the algorithm is to enforce a performance threshold for each evaluation of the black-box function and so is unrelated to our problem definition. In terms of acquisition functions, [23, 24] propose principled approaches to handling aleatoric noise in the homoscedastic setting that could be extended to the heteroscedastic setting. Our primary focus in this work however, is to highlight that heteroscedasticity in the surrogate model is beneficial and so an examination of a subset of acquisition functions is sufficient for this purpose.

# 3 Background

Bayesian optimisation features a surrogate model for the black-box objective. The surrogate model should maintain calibrated uncertainty estimates in order to guide the acquisition of new data points. GPs are often a popular choice of surrogate model in BO applications because of their ability to represent uncertainty.

## 3.1 Gaussian Processes

In the terminology of stochastic processes we may formally define a GP as follows:

**Definition 1.** A Gaussian Process is a collection of random variables, any finite number of which have a joint Gaussian distribution.

The random variables consist of function values $f(\mathbf{x})$ at different locations $\mathbf{x}$ within the design space. The GP is characterised by a mean function

$$m(\mathbf{x}) = \mathbb{E}[f(\mathbf{x})] \tag{1}$$

and a covariance function

$$k(\mathbf{x}, \mathbf{x}') = \mathbb{E}[(f(\mathbf{x} - m(\mathbf{x}))(f(\mathbf{x}') - m(\mathbf{x}'))]. \tag{2}$$

The process is written as follows

$$f(\mathbf{x}) \sim \mathcal{GP}\big(m(\mathbf{x}), k(\mathbf{x}, \mathbf{x}')\big). \tag{3}$$

In our experiments, the prior mean function will be set to the data mean after normalisation of the inputs and standardisation of the outputs. As such, $m(\mathbf{x}) = 0$ will be assumed henceforth. The covariance function computes the pairwise covariance between two random variables (function values). The covariance between a pair of output values $f(\mathbf{x})$ and $f(\mathbf{x}')$ is a function of an input pair $\mathbf{x}$ and $\mathbf{x}'$. As such, the kernel encodes smoothness assumptions about the latent function being modelled; similarity in input space yields outputs that are close [25]. The most widely-utilised kernel is the squared exponential (SE) kernel

$$k_{\text{SQE}}(\boldsymbol{x}, \boldsymbol{x'}) = \sigma_f^2 \cdot \exp\Big(\frac{-\|\boldsymbol{x} - \boldsymbol{x'}\|^2}{2\ell^2}\Big) \tag{4}$$

where $\sigma_f^2$ is the signal amplitude hyperparameter (vertical lengthscale) and $\ell$ is the (horizontal) lengthscale hyperparameter. We use the squared exponential kernel in all experiments. For further information on Gaussian Processes the reader is referred to [26].

## 3.2 Bayesian Optimisation

**Problem Statement** The global optimisation problem is defined as

$$\mathbf{x}^* = \arg\min_{\mathbf{x} \in \mathcal{X}} f(\mathbf{x}) \tag{5}$$

where $\mathbf{x}^*$ is the global optimiser of a black-box function $f : \mathcal{X} \rightarrow \mathcal{Y}$. $\mathcal{X}$ is the design space and is typically a compact subset of $\mathbb{R}^d$. What makes this optimisation problem practically relevant in applications are the following properties:

1. Black-box Objective: We don't have the analytic form of $f$. We can however evaluate $f$ pointwise anywhere in the design space $\mathcal{X}$.
2. Expensive Evaluations: Choosing an input location $\mathbf{x}$ and evaluating $f(\mathbf{x})$ takes a very long time.
3. Noise: The evaluation of a given $\mathbf{x}$ is a noisy process. In addition, this noise may vary across $\mathcal{X}$, making the underlying process heteroscedastic.

We have a dataset of past observations $\mathcal{D} = \{(\boldsymbol{x}_i, t_i)\}_{i=1}^n$ consisting of observations of the black-box function $f$ and fit a surrogate model to these datapoints. We then leverage the predictive mean as well as the uncertainty estimates of the surrogate model to guide the acquisition of the next data point $\boldsymbol{x}_{n+1}$ according to a heuristic known as an acquisition function.

## 4 Heteroscedastic Bayesian Optimisation

We wish to perform Bayesian optimisation whilst minimising input-dependent aleatoric noise. In order to represent input-dependent aleatoric noise, a heteroscedastic surrogate model is required. We take the most likely heteroscedastic GP approach of [27], adopting the notation presented there for consistency. We have a dataset $\mathcal{D} = \{(\mathbf{x}_i, t_i)\}_{i=1}^n$ in which the target values $t_i$ have been generated according to $t_i = f(\mathbf{x}_i) + \epsilon_i$. We assume independent Gaussian noise terms $\epsilon_i \sim \mathcal{N}(0, \sigma_i)$ with variances given by $\sigma_i = r(\mathbf{x}_i)$. In the heteroscedastic setting $r$ is typically a non-constant function over the input domain $\mathbf{x}$. In order to perform Bayesian optimisation, we wish to model the predictive distribution $P(\mathbf{t}^* \mid \mathbf{x}_1^*, \ldots, \mathbf{x}_q^*)$ at the query points $\mathbf{x}_1^*, \ldots, \mathbf{x}_q^*$. Placing a GP prior on $f$ and taking $r(\mathbf{x})$ as the assumed noise rate function, the predictive distribution is multivariate Gaussian $\mathcal{N}(\mu^*, \Sigma^*)$ with mean

$$\mu^* = E[\mathbf{t}^*] = K^*(K + R)^{-1}\mathbf{t} \tag{6}$$

and covariance matrix

$$\Sigma^* = \text{var}[\mathbf{t}^*] = K^{**} + R^* - K^*(K + R)^{-1}K^{*T}, \tag{7}$$

where $K \in \mathbb{R}^{n \times n}$, $K_{ij} = k(\mathbf{x}_i, \mathbf{x}_j)$, $K^* \in \mathbb{R}^{q \times n}$, $K_{ij}^* = k(\mathbf{x}_i^*, \mathbf{x}_j)$, $K^{**} \in \mathbb{R}^{q \times q}$, $K_{ij}^{**} = k(\mathbf{x}_i^*, \mathbf{x}_j^*)$, $\mathbf{t} = (t_1, t_2, \ldots, t_n)^T$, $R = \text{diag}(\mathbf{r})$ with $\mathbf{r} = (r(\mathbf{x}_1), r(\mathbf{x}_2), \ldots, r(\mathbf{x}_n))^T$, and $R^* = \text{diag}(\mathbf{r}^*)$ with $\mathbf{r}^* = (r(\mathbf{x}_1^*), r(\mathbf{x}_2^*), \ldots, r(\mathbf{x}_q^*))^T$.

The most likely heteroscedastic GP algorithm [27] executes the following steps:

1. Estimate a homoscedastic GP, $G_1$ on the dataset $\mathcal{D} = \{(\mathbf{x}_i, t_i)\}_{i=1}^n$
2. Given $G_1$, we estimate the empirical noise levels for the training data using $\text{var}[t_i, G_1(\mathbf{x}_i, \mathcal{D})] = 0.5\,(t_i - \mathbb{E}[x])^2$ forming a new dataset $\mathcal{D}' = \{(\mathbf{x}_i, z_i)\}_{i=1}^n$. A note on the form of this variance estimator is give in Appendix B.
3. Estimate a second GP, $G_2$ on $\mathcal{D}'$.
4. Estimate a combined GP, $G_3$ on $\mathcal{D}$ using $G_2$ to predict the logarithmic noise levels $r_i$.
5. If not converged, set $G_3$ to $G_1$ and repeat.

The Bayesian optimisation problem may be framed as

$$\boldsymbol{x}^* = \underset{\boldsymbol{x} \in \mathcal{X}}{\arg\min}\, f(\boldsymbol{x}), \tag{8}$$

where the black-box objective $f$, to be minimised has the form

$$f(\boldsymbol{x}) = g(\boldsymbol{x}) + s(\boldsymbol{x}). \tag{9}$$

$s(\boldsymbol{x})$ is, in this instance, the true noise rate function. We investigate extensions of the expected improvement [28] acquisition criterion, the principal form of which may be written in terms of the targets $t$ and the incumbent best objective function value, $\eta$, found so far as

$$\text{EI}(\boldsymbol{x}) = \mathbb{E}\big[\,(\eta - t)_+\big] = \int_{-\infty}^{\infty} (\eta - t)_+ \, p(t \,|\, \boldsymbol{x}) \, dt \tag{10}$$

where $p(t \,|\, \boldsymbol{x})$ is the posterior predictive marginal density of the objective function evaluated at $\boldsymbol{x}$. $(\eta - t)_+ \equiv \max\,(0,\ \eta - t)$ is the improvement over the incumbent best objective function value $\eta$.

We propose two extensions to the expected improvement criterion. The first is an extension of the augmented expected improvement criterion

$$\text{AEI}(\boldsymbol{x}) = \mathbb{E}\big[(\eta - t)_+\big]\left(1 - \frac{\sigma_n}{\sqrt{\text{var}[\mathbf{t}^*] + \sigma_n^2}}\right), \tag{11}$$

of [29] where $\sigma_n$ is the fixed aleatoric noise level. We extend AEI to the heteroscedastic setting by exchanging the fixed aleaotric noise level with the input-dependent one:

$$\text{het-AEI}(\boldsymbol{x}) = \mathbb{E}\big[(\eta - t)_+\big]\left(1 - \frac{\sqrt{r(\boldsymbol{x})}}{\sqrt{\text{var}[\mathbf{t}^*] + r(\boldsymbol{x})}}\right). \tag{12}$$

where $r(\boldsymbol{x})$ is the predicted aleatoric uncertainty at input $\boldsymbol{x}$ under the most likely heteroscedastic GP and var$[\mathbf{t}^*]$ is the predictive variance of the heteroscedastic GP incorporating both aleatoric and epistemic components of the uncertainty. We also propose a simple modification to the expected improvement acquisition function that explicitly penalises regions of the input space with large aleatoric uncertainty. We call this acquisition function aleatoric noise-penalised expected improvement (ANPEI) and denote it

$$\text{ANPEI} = \alpha \text{EI}(\boldsymbol{x}) - (1 - \alpha)\sqrt{r(\boldsymbol{x})} \tag{13}$$

where $\alpha$ is a scalarisation constant which we set to $0.5$ for the experiments in this paper. In the multiobjective optimisation setting a particular value of $\alpha$ will correspond to a point on the Pareto frontier. We use both the modification to AEI (het-AEI) and ANPEI acquisition function in conjunction with the most likely heteroscedastic GP surrogate model in the experiments that follow.

# 5 Experiments

## 5.1 Implementation

Experiments were run using a custom implementation of Gaussian Process regression and most likely heteroscedastic Gaussian Process regression. The code is publicly available at `https://github.com/Ryan-Rhys/Heteroscedastic-BO`. The squared exponential kernel was chosen as the covariance function for both the homoscedastic GP as well as $G_1$ and $G_2$ of the most likely heteroscedastic GP. The lengthscales, $\ell$, of the homoscedastic GP were initialised to 1.0 for each input dimension across all toy problems after standardisation of the output values following the recommendation of [30]. The signal amplitude $\sigma_f^2$ was initialised to a value of 2.5. The lengthscale, $\ell$, of $G_2$ of the most likely heteroscedastic GP [27] was initialised to 1.0, the initial noise level of $G_2$ was set to 1.0. The EM-like procedure required to train the most likely heteroscedastic GP was run for 10 iterations and the sample size required to construct the variance estimator producing the auxiliary dataset was 100. Hyperparameter values were obtained by optimising the marginal likelihood using the scipy implementation of the L-BFGS optimiser.

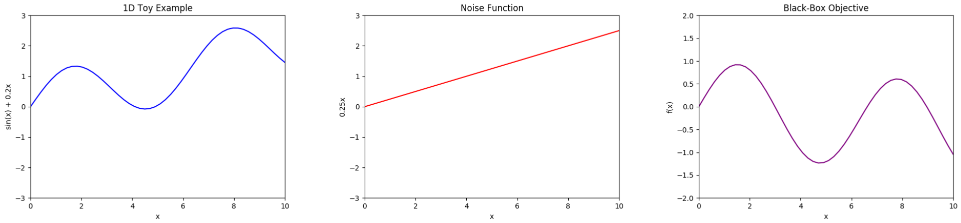

(a) 1D Toy Objective (b) Noise Rate Function (c) Black-box Objective

Figure 3: Toy 1D Problem. The toy objective in a) is corrupted with heteroscedastic noise according to the function in b). The combined objective, which when optimised maximises the sin wave subject to the minimisation of aleatoric noise, is given in c) and is obtained by subtracting the noise function from the 1D sinusoid.

### 5.2 1D Toy Objective with Linear Noise Rate Function

Referring to Equation 9 from section 4, in the first experiment we take a one-dimensional sin wave

$$g(x) = \sin(x) + 0.2(x) \tag{14}$$

with noise rate function $s(x) = 0.25x$. These functions as well as the black-box objective $f(x)$ are shown in Figure 3. The Bayesian optimisation problem is designed such that the first maximum in 3(a) is to be preferred as samples from this region of the input space will have a smaller noise rate. The black-box objective in 3(c) illustrates this trade-off. In 5(a) we compare the performance of a Bayesian optimisation scheme involving a vanilla GP in conjunction with the EI acquisition function with the most likely heteroscedastic GP in conjunction with the ANPEI and AEI acquisition functions. The experiment is designed to contrast the performance of a standard Bayesian optimisation scheme against our approach in a situation where minimising aleatoric noise is desirable.

### 5.3 Branin-Hoo with Non-linear Noise Rate Function

In the second experiment we consider the Branin-Hoo function as $g(\boldsymbol{x})$ with a non-linear noise rate function given by $s(\boldsymbol{x}) = 1.4{x_1}^2 + 0.3x_2$. Given that this example is a minimisation problem, the black-box objective consists of the sum of the Branin-Hoo function and the noise rate function. Contour plots of the functions are shown in Figure 4. A comparison, in terms of the best objective function values found, between the vanilla GP and EI acquisition function with the most likely heteroscedastic GP and ANPEI and AEI acquisition functions is given in 5(b).

### 5.4 Optimising the Phosphorus Fraction of Soil

In this real-world problem we apply heteroscedastic Bayesian optimisation to the problem of optimising the phosphorus fraction of soil. Soil phosphorus is an essential nutrient for plant growth and is widely used as a fertiliser in agriculture. While the amount of arable land worldwide is declining, global population is expanding and so is demand of food. As such, understanding the availability of plant nutrients that increase crop yield is essential. To this end, [31] have curated a dataset on soil phosphorus, relating phosphorus content to variables including soil particle size, total nitrogen, organic carbon and bulk density. In this experiment, we study the relationship between bulk soil density and the phosphorus fraction, the goal being to minimise the phosphorus content of soil subject to heteroscedastic noise. We provide evidence that there is heteroscedasticity in the problem by comparing the fits of a homoscedastic GP and the most likely heteroscedastic GP in Figure 2 and provide a predictive performance comparison based on negative log predictive density values in the appendix. In this problem we don't have access to a continuous-valued black-box function or a ground truth noise function. As such, the surrogate models were initialised with a subset of the data and the query locations selected by Bayesian optimisation were mapped to the closest data points in the heldout data. Our procedure for generating pseudo ground truth noise values was to:

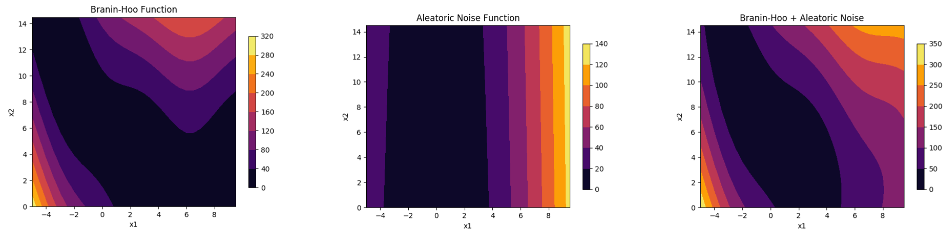

(a) 2D Branin-Hoo Function (b) Non-linear Noise Function (c) Black-box Objective

Figure 4: Toy 2D Problem. The Branin-Hoo objective function in a) is corrupted by the heteroscedastic noise function in b) $s(x_1, x_2) = 1.4{x_1}^2 + 0.3x_2$. The black-box objective function c) is obtained by summing the functions in a) and b). The sum is required to penalise regions of large aleatoric noise because the objective is being minimised.

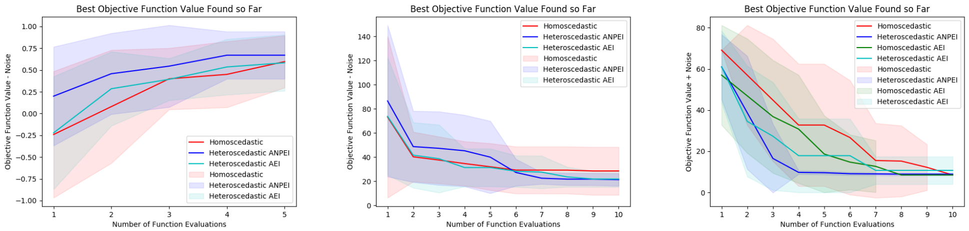

(a) 1D Toy Objective (b) 2D Branin-Hoo (c) Soil Phosphorus Fraction

Figure 5: Results of heteroscedastic and homoscedastic Bayesian optimisation on the 3 problems considered. Error bars are computed using 10 random initialisations.

1. Fit a homoscedastic GP to the full dataset
2. At each point $x_i$, compute the corresponding square error $s_i^2 = (y_i - \mu(x_i))^2$
3. Estimate variances by computing a moving average of the squared errors, where the relative weight of each $s_i^2$ was assigned with a Gaussian kernel.

The performances of homoscedastic Bayesian optimisation using EI and AEI and heteroscedastic Bayesian optimisation using ANPEI and AEI are compared in 5(c).

### 5.5 Discussion

In all experiments the most likely heteroscedastic GP and ANPEI combination/heteroscedastic AEI combination outperform the homoscedastic GP and EI. The fact that the homoscedastic GP has no knowledge of the heteroscedasticity of the noise rate function puts it at a serious disadvantage. In the first sin wave problem, designed to highlight this point, the heteroscedastic Bayesian optimisation scheme consistently and preferentially finds the first maximum as that which minimises aleatoric noise. In contrast the homoscedastic GP, finds it impossible to differentiate between the two maxima. The experiments provide strong evidence that modelling heteroscedasticity in Bayesian optimisation is a more flexible approach to assuming homoscedastic noise.

## 6 Conclusion and Future Work

We have presented an approach for performing Bayesian optimisation with the explicit goal of minimising aleatoric uncertainty in the suggestions. We posit that such an approach can prove useful for the natural sciences in the search for molecules and materials that are robust to experimental noise. We demonstrate concrete improvements on one and two-dimensional toy problems as well as a real-world optimisation problem and contribute an open-source implementation of the most likely heteroscedastic GP as a surrogate model for Bayesian optimisation. In future work we plan to apply our approach to molecular property optimisation [4]. To this end it would be useful to investigate the potential for replicates to improve the heteroscedastic BO scheme [32, 33, 34]. Furthermore it may be possible to leverage recent advances in combinatorial Bayesian optimisation [35, 36, 37] in order to perform heteroscedastic Bayesian optimisation over molecular graphs.

# References

[1] Rafael Gómez-Bombarelli, Jennifer N Wei, David Duvenaud, José Miguel Hernández-Lobato, Benjamín Sánchez-Lengeling, Dennis Sheberla, Jorge Aguilera-Iparraguirre, Timothy D Hirzel, Ryan P Adams, and Alán Aspuru-Guzik. Automatic chemical design using a data-driven continuous representation of molecules. *ACS Central Science*, 4(2):268–276, 2018.

[2] Ryan-Rhys Griffiths and José Miguel Hernández-Lobato. Constrained Bayesian optimization for automatic chemical design. *arXiv preprint arXiv:1709.05501*, 2017.

[3] Omar Mahmood and José Miguel Hernández-Lobato. A cold approach to generating optimal samples. *arXiv preprint arXiv:1905.09885*, 2019.

[4] Ksenia Korovina, Sailun Xu, Kirthevasan Kandasamy, Willie Neiswanger, Barnabas Poczos, Jeff Schneider, and Eric P Xing. Chembo: Bayesian optimization of small organic molecules with synthesizable recommendations. *arXiv preprint arXiv:1908.01425*, 2019.

[5] Tristan Aumentado-Armstrong. Latent molecular optimization for targeted therapeutic design. *arXiv preprint arXiv:1809.02032*, 2018.

[6] Jialin Song, Yury S. Tokpanov, Yuxin Chen, Dagny Fleischman, Kate T. Fountaine, Harry A. Atwater, and Yisong Yue. Optimizing Photonic Nanostructures via Multi-fidelity Gaussian Processes. *arXiv:1811.07707 [cs, stat]*, November 2018.

[7] Jialin Song, Yuxin Chen, and Yisong Yue. A general framework for multi-fidelity bayesian optimization with gaussian processes. In *The 22nd International Conference on Artificial Intelligence and Statistics*, pages 3158–3167, 2019.

[8] Henry C Herbol, Weici Hu, Peter Frazier, Paulette Clancy, and Matthias Poloczek. Efficient search of compositional space for hybrid organic–inorganic perovskites via Bayesian optimization. *npj Computational Materials*, 4(1):51, 2018.

[9] Roberto Calandra, André Seyfarth, Jan Peters, and Marc Peter Deisenroth. Bayesian optimization for learning gaits under uncertainty. *Annals of Mathematics and Artificial Intelligence*, 76 (1-2):5–23, 2016.

[10] James Grant, Alexis Boukouvalas, Ryan-Rhys Griffiths, David Leslie, Sattar Vakili, and Enrique Munoz De Cote. Adaptive sensor placement for continuous spaces. In *Proceedings of the 36th International Conference on Machine Learning*, volume 97 of *Proceedings of Machine Learning Research*, pages 2385–2393, Long Beach, California, USA, 09–15 Jun 2019. PMLR.

[11] Simon Olofsson, Mohammad Mehrian, Roberto Calandra, Liesbet Geris, Marc Peter Deisenroth, and Ruth Misener. Bayesian multiobjective optimisation with mixed analytical and black-box functions: Application to tissue engineering. *IEEE Transactions on Biomedical Engineering*, 66(3):727–739, 2018.

[12] Guilherme Duarte Ramos Matos, Daisy Y Kyu, Hannes H Loeffler, John D Chodera, Michael R Shirts, and David L Mobley. Approaches for calculating solvation free energies and enthalpies demonstrated with an update of the freesolv database. *Journal of Chemical & Engineering Data*, 62(5):1559–1569, 2017.

[13] Ryan-Rhys Griffiths, Philippe Schwaller, and Alpha A. Lee. Dataset bias in the natural sciences: A case study in chemical reaction prediction and synthesis design. *ChemRxiv*, 2018.

[14] José Miguel Hernández-Lobato, James Requeima, Edward O Pyzer-Knapp, and Alán Aspuru-Guzik. Parallel and distributed thompson sampling for large-scale accelerated exploration of chemical space. In *International Conference on Machine Learning*, pages 1470–1479, 2017.

[15] Roberto Calandra. *Bayesian Modeling for Optimization and Control in Robotics*. PhD thesis, Technische Universität, 2017.

[16] Miguel Lázaro-Gredilla and Michalis K Titsias. Variational heteroscedastic Gaussian process regression. In *Proceedings of the 28th International Conference on International Conference on Machine Learning*, pages 841–848. Omnipress, 2011.

[17] Scott R Kuindersma, Roderic A Grupen, and Andrew G Barto. Variable risk control via stochastic optimization. *The International Journal of Robotics Research*, 32(7):806–825, 2013.

[18] John-Alexander M Assael, Ziyu Wang, Bobak Shahriari, and Nando de Freitas. Heteroscedastic treed Bayesian optimisation. *arXiv preprint arXiv:1410.7172*, 2014.

[19] Ryo Ariizumi, Matthew Tesch, Howie Choset, and Fumitoshi Matsuno. Expensive multiobjective optimization for robotics with consideration of heteroscedastic noise. In *2014 IEEE/RSJ International Conference on Intelligent Robots and Systems*, pages 2230–2235. IEEE, 2014.

[20] Zilong Wang and Marianthi Ierapetritou. A novel surrogate-based optimization method for black-box simulation with heteroscedastic noise. *Industrial & Engineering Chemistry Research*, 56(38):10720–10732, 2017.

[21] Yanan Sui, Alkis Gotovos, Joel Burdick, and Andreas Krause. Safe exploration for optimization with Gaussian processes. In *International Conference on Machine Learning*, pages 997–1005, 2015.

[22] Felix Berkenkamp, Andreas Krause, and Angela P. Schoellig. Bayesian optimization with safety constraints: Safe and automatic parameter tuning in robotics. *ArXiv*, abs/1602.04450, 2016.

[23] Peter Frazier, Warren Powell, and Savas Dayanik. The knowledge-gradient policy for correlated normal beliefs. *INFORMS journal on Computing*, 21(4):599–613, 2009.

[24] Benjamin Letham, Brian Karrer, Guilherme Ottoni, Eytan Bakshy, et al. Constrained Bayesian optimization with noisy experiments. *Bayesian Analysis*, 14(2):495–519, 2019.

[25] Pedro M Domingos. A few useful things to know about machine learning. *Commun. acm*, 55 (10):78–87, 2012.

[26] C. E. Rasmussen and C. K. I. Williams. *Gaussian Processes for Machine Learning*. MIT Press, 2006.

[27] Kristian Kersting, Christian Plagemann, Patrick Pfaff, and Wolfram Burgard. Most likely heteroscedastic Gaussian process regression. In *Proceedings of the 24th International Conference on Machine Learning - ICML '07*, pages 393–400, Corvalis, Oregon, 2007. ACM Press. ISBN 978-1-59593-793-3. doi: 10.1145/1273496.1273546.

[28] Donald R Jones, Matthias Schonlau, and William J Welch. Efficient global optimization of expensive black-box functions. *Journal of Global optimization*, 13(4):455–492, 1998.

[29] Deng Huang, Theodore T Allen, William I Notz, and Ning Zeng. Global optimization of stochastic black-box systems via sequential kriging meta-models. *Journal of global optimization*, 34(3):441–466, 2006.

[30] Iain Murray. Introduction to Gaussian processes. 2008.

[31] Enqing Hou, Xiang Tan, Marijke Heenan, and Dazhi Wen. A global dataset of plant available and unavailable phosphorus in natural soils derived by Hedley method. *Scientific Data*, 5(1): 180166, December 2018. ISSN 2052-4463. doi: 10.1038/sdata.2018.166.

[32] Alexis Boukouvalas and Dan Cornford. Learning heteroscedastic Gaussian processes for complex datasets. *Technical report*, 2009.

[33] Mickael Binois, Robert B Gramacy, and Mike Ludkovski. Practical heteroscedastic Gaussian process modeling for large simulation experiments. *Journal of Computational and Graphical Statistics*, 27(4):808–821, 2018.

[34] Mickaël Binois, Jiangeng Huang, Robert B Gramacy, and Mike Ludkovski. Replication or exploration? sequential design for stochastic simulation experiments. *Technometrics*, 61(1): 7–23, 2019.

[35] Ricardo Baptista and Matthias Poloczek. Bayesian optimization of combinatorial structures. In *International Conference on Machine Learning*, pages 462–471, 2018.

[36] Changyong Oh, Jakub M Tomczak, Efstratios Gavves, and Max Welling. Combinatorial Bayesian optimization using graph representations. *arXiv preprint arXiv:1902.00448*, 2019.

[37] Poompol Buathong, David Ginsbourger, and Tipaluck Krityakierne. Kernels over sets of finite sets using RKHS embeddings, with application to Bayesian (combinatorial) optimization. *arXiv preprint arXiv:1910.04086*, 2019.

# A Heteroscedasticity of the Soil Phosphorus Fraction Dataset

Table 1 is used to demonstrate the efficacy of modelling the soil phosphorus fraction dataset using a heteroscedastic GP. The heteroscedastic GP outperforms the homoscedastic GP on prediction based on the metric of negative log predictive density (NLPD)

$$\text{NLPD} = \frac{1}{n} \sum_{i=1}^{n} - \log p(t_i | \boldsymbol{x_i}) \tag{15}$$

which penalises both over and under-confident predictions.

Table 1: Comparison of NLPD values on the soil phosphorus fraction dataset. Standard errors are reported for 10 independent train/test splits.

| **Soil Phosphorus Fraction Dataset** | **GP** | **Het GP** |
|---|---|---|
| NLPD | $1.35 \pm 1.33$ | $1.00 \pm 0.95$ |